Accepted Manuscript

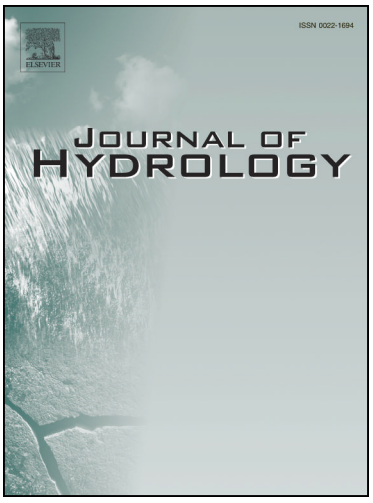

Research papers

Influence of the β parameter of the Haverkamp model on the transient soil water infiltration curve

B. Latorre, D. Moret-Fernández, L. Lassabatere, M. Rahmati, M.V. López, R. Angulo-Jaramillo, R. Sorando, F. Comín, J.J. Jiménez

PII: S0022-1694(18)30511-0
DOI: https://doi.org/10.1016/j.jhydrol.2018.07.006
Reference: HYDROL 22938

To appear in: *Journal of Hydrology*

Received Date: 24 April 2018
Revised Date: 5 June 2018
Accepted Date: 2 July 2018

Please cite this article as: Latorre, B., Moret-Fernández, D., Lassabatere, L., Rahmati, M., López, M.V., Angulo-Jaramillo, R., Sorando, R., Comín, F., Jiménez, J.J., Influence of the β parameter of the Haverkamp model on the transient soil water infiltration curve, *Journal of Hydrology* (2018), doi: https://doi.org/10.1016/j.jhydrol.2018.07.006

This is a PDF file of an unedited manuscript that has been accepted for publication. As a service to our customers we are providing this early version of the manuscript. The manuscript will undergo copyediting, typesetting, and review of the resulting proof before it is published in its final form. Please note that during the production process errors may be discovered which could affect the content, and all legal disclaimers that apply to the journal pertain.

Influence of the β parameter of the Haverkamp model on the transient soil water infiltration curve

B. Latorre [a], D. Moret-Fernández [a] *, Lassabatere[b] , L., M. Rahmati [c], M.V. López [a], R. Angulo-Jaramillo[b], R. Sorando [d], F. Comín [d], J.J. Jiménez [e]

[a] Departamento de Suelo y Agua, Estación Experimental de Aula Dei, Consejo Superior de Investigaciones Científicas (CSIC), PO Box 13034, 50080 Zaragoza, Spain.

[b] Université de Lyon; UMR5023 Laboratoire d'Ecologie des Hydrosystèmes Naturels et Anthropisés; Université Lyon 1; ENTPE; CNRS; 3, rue Maurice Audin, 69518 Vaulx-en-Velin, France

[c] Department of Soil Science, Faculty of Agriculture, University of Maragheh, Iran.

[d] Instituto Pirenaico de Ecología-CSIC. Av. Montañana 1005. 50059 Zaragoza. Spain

[e] ARAID. Pyrenean Institute of Ecology (IPE-CSIC) Avda. Ntra. Sra. de la Victoria 16 Jaca 22700 (Huesca) Spain

* Corresponding author. E-mail: david@eead.csic.es Tel.: (+34) 976 71 61 40

ABSTRACT

Soil water infiltration can be described with the quasi-analytical Haverkamp et al. (1994) equation, defined by the hydraulic conductivity (K_s), sorptivity (S) and the β parameter. K_s and S are commonly estimated from the transient cumulative infiltration curve, using a constant β value. The objective of this work was to study the influence of β on the estimation of K_s and S. The study was first performed on synthetic 1-D infiltration curves generated at different infiltration times for loam sandy, loamy and silty soils, and next extrapolated to a 3-D loam synthetic soil and on 10 infiltrations curves measured on the field with a disc infiltrometer on different types of soils. The infiltration measurements lasted between 600 and 900 s. The results showed that, while early infiltration times (i.e. 100 s) promoted good estimations for S, longer infiltrations (i.e. 1.000s) were required to estimate accurately K_s. Only very long infiltration (i.e. 10.000 s) allowed defining the actual β value. A similar behaviour was observed for the 3-D infiltration measurements. Except for β, significant relationships (R^2 = 0.99) were obtained between the K_s and S of the three theoretical soils and the corresponding values calculated by optimizing the three hydraulic parameters on 2.000 s 1-D infiltration curves. The large confidence interval observed in β (between 0.3 and 2.0) resulted from the fact that β had a small effect on the infiltration curve. A significant relationship (R^2 = 0.99) was also obtained between the K_s and S optimized from the exprimental curves using a β = 1.1 and the corresponding values obtained by simultaneous optimization of the three hydraulic parameters. These results demonstrated that S and K_s can be accurately estimated using a constant β and that downward infiltration is not an appropriate procedure to estimate β.

Keywords: Sorptivity, Hydraulic Conductivity; Water Retention Curve, Methods

1.- INTRODUCTION

The knowledge of water movement in the soil is of central importance in many research areas, such as agronomy, civil engieneering, hydrology and environmental sciences. Haverkamp et al. (1994) developed a physical base three-dimensional infiltration model for disc infiltrometer derived from the Richards equation. This equation was the sum of the 1-D infiltration curve, defined by the hydraulic conductivity (K), sorptivity (S) and the β parameter, and an additional term depending on time, the disc radius, the initial and final soil volumetric water contents, the S value and a proportionality constant (γ). The complete Haverkamp et al. (1994) model, together with its approximate expansions, have been successfully applied in many different infiltration researches (Pueyo et al., 2013; Moret-Fernández et al., 2013; Latorre et al., 2015; Di Prima et al., 2016; among others). In particular, the approximate expansions for the transient and steady states are used in many methods designed for the hydraulic characterization of soil (e.g., Lassabatere et al., 2006, Yilmaz et al., 2010; Bagarello et al., 2014).

Sorptivity describes the capacity of a porous medium to absorb or desorb liquid (Philip, 1957). It is a function of the diffusivity and the initial and final volumetric water content (θ) (Parlange et al., 1975). K, which measures the soil ability to transmit water when it is submitted to a hydraulic gradient, is function of the hydraulic head or the soil water content (Dane and Hopmans, 2002). β is an integral shape constant that depends on the soil diffusivity, the hydraulic conductivity function, and the initial and final volumetric water contents (Haverkamp et al., 2006). Within the applicability of the model, β ranges between 0.3 and 1.7, suitable from sandy to silty soil textures, as estimated by Lassabatere et al. (2009), using numerically generated data. Recent works demonstrated that β is related to the soil textural characteristics (Moret-Fernández et al., 2017). γ is a correction factor for the use of simplified geometry of the wetting front below disc infiltrometer to derive the additional term for 3D infiltration (Haverkamp et al., 1994). Although Fuentes et al. (1992) proposed physically based equations to define parameters β and γ, Lassabatere et al. (2009) observed that their

formulations provided values contrasting with actual and plausible values. These same authors found that γ was dependent on the soil type, with values ranging between 0.75 and 1. More recently, Latorre et al. (2015) compared the complete Haverkamp et al. (1994) formulation with synthetic infiltration curves generated with HDYRUS-2D, and observed that consistent K and S values were obtained from inverse analysis of these cumulative infiltration curves when constant β and γ values were employed. In this case, the constant γ value of 0.75 proposed by Haverkamp et al. (1994) will be used. The study of this parameter will be the subject of further studies, and the proposed study focuses on the role played by parameter β, with the analysis of its impact on 1D cumulative infiltration curves or 3D infiltration curves computed considering parameter γ fixed at 0.75. Further research will focus on the addition of parameter γ as potentially variable and optimizable.

Infiltration-based methods are valuable techniques to measure the soil hydraulic properties. Among the different infiltration-instruments, the tension disc infiltrometer is a worldwide used tool for in situ estimation of soil hydraulic properties in the vadose zone. This instrument consists of a base disc jointed to a graduated water-supply reservoir and a bubble tower to impose a negative pressure head (h) at the base disc (Perroux and White, 1988). The soil hydraulic properties are commonly calculated from the cumulative water infiltration curves, which are measured from the drop in the water level of the reservoir tower. Correct measurements of the infiltration curve require the membrane of the disc base to be completely in contact with the soil surface. To achieve this, a contact sand layer is placed on the soil surface. Several procedures have been developed to estimate K and S from tension disc infiltrometer measurements, including the analysis of (i) the steady-state data (Smettem and Clothier, 1989; Ankeny et al., 1991), (ii) the early-medium transient state curve (e.g. Vandervaere et al., 2000), (iii) the combination of transient and steady states (Lassabatere et al., 2006); and (iv) the whole cumulative infiltration curve (Latorre et al., 2015). Compared to the steady-state water flow methods, the transient water flow procedures, that require shorter experiments and ensure smaller sampled soil volumes and more homogeneous initial water distribution, lead to better estimates and better

representativeness of the local hydraulic properties (Angulo-Jaramillo et al., 2000). On the other hand, comparing different transient methods, Latorre et al. (2015) demonstrated that the use of the complete quasi-analytical Haverkamp et al. (1994) equation gives more robust results than the methods based on the simplified Haverkamp et al. (1994) formulation. However, in both cases a constant β value is employed. Although Haverkamp et al. (1994) and Latorre et al. (2015) supported this assumption, several studies have proved that the parameter β was not necessarily constant and could vary with the type of soil (Moret-Fernández and Latorre, 2017, Lassabatere et al., 2009).

Given the above-described studies, which show that the effect of β on the estimation of downward infiltration is not clear enough, the objective of this paper is to deepen the study of the Haverkamp equation by analysing the influence of β on the downward infiltration curve and related consequences when inverting the downward infiltration curves to derive soil hydraulic parameters. Because of its greater simplicity, the analysis was first applied on synthetic 1-D infiltration curves, and next extrapolated to 3-D synthetic and experimental infiltration curves measured with a disc infiltrometer.

2. METHOD AND MATERIALS

2.1. Theory

The 1-D cumulative infiltration, I_{1D}, is described by the quasi-exact equation, derived by Haverkamp et al. (1994) from the Richards equation:

$$\frac{2\left(K_0-K_i\right)^2}{S_0^2}t=\frac{2}{1-\beta}\frac{\left(K_0-K_i\right)\left(I_{1D}-K_it\right)}{S_0^2}-\frac{1}{1-\beta}\cdot\ln\left[\frac{1}{\beta}\exp\left(2\beta\left(K_0-K_i\right)\left(I_{1D}-K_it\right)/S_0^2\right)+\frac{\beta-1}{\beta}\right] \quad (1)$$

where t is time (T), K_0 and K_i (L T^{-1}) are the hydraulic conductivity values corresponding to the final, θ_0, and initial, θ_i, volumetric water content (L^{-3} L^{-3}), respectively; S_0 (L $T^{-0.5}$) is the sorptivity for θ_0 (L^3 L^{-3}); and β is defined as an integral shape parameter.

The 3-D cumulative infiltration, I_{3D}, from a surface disc source can be expressed by the 1-D equation plus an additional time linear term (Smettem et al., 1994):

$$I_{3D} = I_{1D} + \frac{\gamma S_0^2}{R_D\left(\theta_0 - \theta_i\right)} t \tag{2}$$

where R_D (L) is the radius of the disc and γ is the proportionality constant. Substituting Eq. (2) into Eq. (1), an implicit 3-D infiltration equation valid for the entire time range is obtained (Haverkamp et al., 1994)

$$\frac{2\left(K_0 - K_i\right)^2}{S_0^2} t = \frac{2}{1-\beta} \frac{\left(K_0 - K_i\right)\left[I_{3D} - K_i t - \gamma S_0^2 / \left(\left(\theta_0 - \theta_i\right) R_D\right) t\right]}{S_0^2} -$$

$$\frac{1}{1-\beta} \cdot \ln\left[\frac{1}{\beta} \exp\left(2\beta\left(K_0 - K_i\right)\left[I_{3D} - K_i t - \gamma S_0^2 / \left(\left(\theta_0 - \theta_i\right) R_D\right) t\right] / S_0^2\right) + \frac{\beta - 1}{\beta}\right] \tag{3}$$

According to Lassabatere et al. (2009), the values of γ and β range from 0.75 to 1 and from 0.3 to 1.7, respectively, suitable from sandy to silty soils. These authors derived such values by fitting equations (1) and (2) to numerically generated data. The respective initial and boundary conditions for infiltration process are

$$\begin{aligned} &z = 0, t > 0, \theta = \theta_s \\ &|z| \le 0, t = 0, \theta = \theta_i \\ &|z| \to -\infty, t > 0, \theta = \theta_i \end{aligned} \tag{4}$$

where z is a vertical coordinate (L) positive upward and θ_i and θ_s ($L^3\ L^{-3}$) are the initial and saturated volumetric water contents. Depending on the sign of z, downward ($z < 0$) or upward ($z > 0$) infiltration can be described. Fuentes et al. (1992) designed the following estimate forthe β shape coefficient :

$$\beta = 2 - 2\frac{\int_{\theta_i}^{\theta_0} \left(K - K_i / K_0 - K_i\right)\left(\theta_0 - \theta_i / \theta - \theta_i\right) D\left(\theta\right) d\theta}{\int_{\theta_i}^{\theta_0} D\left(\theta\right) d\theta} \tag{5}$$

where $D(\theta)$ ($L^2\ T^{-1}$) is the diffusivity defined by Klute (1952) as

$$D(\theta) = K(\theta)\frac{dh}{d\theta} \tag{6}$$

and h is the matric component of soil water potential (L).

Studying water infiltration into a homogeneous with a uniform initial water content and infinite length horizontal soil column, Parlange (1975) obtained the following estimate for the soil sorptivity:

$$S^2(\theta) = \int_{\theta_i}^{\theta_0} [\theta_0 - \theta][2K - \dots] \tag{7}$$

On the other hand, the unsaturated soil hydraulic properties can be described according to the van Genuchten-Mualem model (Mualem, 1976; van Genuchten, 1980):

$$S_e(h) = \frac{\theta(h) - \theta_r}{\theta_s - \theta_r} = \frac{1}{\left(1 + |\alpha h|^n\right)^m} \tag{8}$$

$$K(\theta) = K_s S_e^{0.5}\left[1 - \left(1 - S_e^{1/m}\right)^m\right]^2 \tag{9}$$

where S_e is the effective water content, θ_r ($L^3\ L^{-3}$) denotes the residual volumetric water content and α (L^{-1}), n, and m=(*1-1/n*) are empirical parameters. Combining Eq. (6), (8) and (9), the diffusivity can be defined as (van Genuchten, 1980):

$$D(S_e) = \frac{(1-m)K_s}{\alpha m(\theta_s - \theta_r)} S_e^{1/2 - 1/m}\left[\left(1 - S_e^{1/m}\right)^{-m} + \left(1 - S_e^{1/m}\right)^m - 2\right] \tag{10}$$

2.2. Estimate of *S*, β and *K* from the inverse analysis of an infiltration curve

Latorre et al. (2015) provided a numerical procedure to solve Eq.(1) and Eq.(3). Since γ is not studied in this work, a constant value equal to 0.75 has been considered (Haverkamp et al., 1994). The S, K and β parameters are estimated by minimizing an objective function, Q, that represents the difference between Eq. (1) or (3) and the experimental cumulative downward infiltration curve:

(11)

where N is the number of measured (I,t) values. To simplify the study, the existence and the uniqueness of the solution was studied by analysing the Q error maps for the K_s-β, S-β and S-K_s planes, where the third parameter of each 2D-map was fixed to the remaining theoretical value (Table 1). A global optimization (Pardalos and Romeijn, 2002) for different infiltration periods was employed.. The response surfaces were calculated on a rectangular grid with K_s from 0.001 to 0.1 mm s^{-1}, S from 0.1 to 1.5 and β ranging from 0.3 to 1.7. An additional analysis of the K_s, S and β with respect to the final time of infiltration was also performed. This consisted on calculating the t-K_s, t-S and t-β error maps using in each plane the theoretical remaining parameters and t ranging from 0 to the end of the infiltration.

In order estimate S, K and β from the inverse analysis of an infiltration curve, a global optimization approach over three dimensions of Q (K_s, S and β) was developed. This optimization process presents the following steps : :

1. The measured data (recorded every 1 s) was resampled to 100 points. To this end, an iterative procedure that determines the error of the regression line for each three consecutive points and removes the central point with lower error, was applied.
2. A three steps global optimization on (S, K_s and β) was preformed: the first one used a (400x50x50) grid, the second one a (100x100x100) grid centered on the optimal S value and

a third one with a (1x400x400) grid on the optimized *S*. The initial grid used for K_s, *S* and β ranged from 0.001 to 0.1 mm s^{-1}, 0.1 to 1.5 mm $s^{-0.5}$ and 0.3 to 1.7, respectively.

3. Within the global search, the simulated curves with a total cumulative infiltration larger/lower than ±5 mm around the experimental value were discarded. This allowed a faster screening of the optimal K_s, *S* and β.

2.3. Numerical experiments

The theoretical downward infiltration data was numerically generated with the HYDRUS-1D and 3-D software (Simunek et al., 2006). Loam sandy, loamy and silty soils (Carsel and Parrish, 1988) were used. The values of the hydraulic parameters (α, *n*, K_s, β and *S*) of the theoretical soils are summarised in Table 1. For 1-D infiltration analysis, a 30 cm-high soil column was discretized using a 1-D mesh of 1000 cells. The minimum time step used in the simulations was 10^{-4} s. The initial pressure head of the homogeneous and isotropic column was -1.66 x10^6 cm, which according to Munkholm and Kay (2002) it corresponds to air-dry conditions. The tension at the base of the soil column was 0 cm. Atmospheric conditions with a maximal tension of 0 cm was imposed at the top boundary. This condition does not allow water to build up on the surface, preventing water overpressures on the soil surface. Since the experimental measurements are relatively fast (between some minutes to 1 h), a null evaporation rate was considered.

The 3-D infiltration experiments were simulated using HYDRUS-3D model (Simunek et al., 1999), considering only a loam soil (Table 1). The soil volume was discretized as a cylinder (radius of 25 cm and depth of 25 cm), covering the axisymmetric plane with a 2-D rectangular mesh of 100×900 cells. The vertical cell size was variable to obtain a finer mesh near the surface, ranging from 0.003 cm on the top to 0.3 cm on the bottom. Maximum and minimum time steps were fixed at 0.05 s and 10^{-4} s, respectively. An initial pressure head of -1.66 x10^6 cm was also selected. This values ensured low initial water contents, θ_i, with $\theta_i < \theta_s$, where θ_s stands for the saturated water

content. The initial soil water content was close to the residual water content. A base disc infiltrometer of 10 cm radius was represented as a constant pressure head boundary on the corresponding cells, the rest of the soil surface was treated as atmospheric boundary with no flux. A null pressure head was considered as bottom and lateral boundaries, which is supposed valid if the water does not reach these regions. Because Eq. (1) the considers the soil as column of infinite length, only the infiltration curves between time zero and the time just before the wetting front arrives to the bottom of the soil column were considered. It was then considered the modeled cumulative infiltration at surface would have been the same for other boundary conditions.. The simulations run up to 50 mm water infiltration.

Under hypothetical perfect downward infiltration curves, the three hydraulic parameters can be optimized up to a very small error (i.e, 10^{-6} mm). However, as reported by Latorre et al. (2015), under experimental conditions the measured infiltration curve is subjected to experimental uncertainties (such as the accuracy of water level measurement). The uncertainty for the experimental disc infiltrometer was 0.05 mm, which means the lowest contour line should correspond to an uncertainty of 0.05 mm for the distance between the fitted and target cumulative infiltrations. Therefore, a well-shaped contour line corresponding to 0.05 mm confirms that there should be only one unique solution for applied method while the contour line with a valley shape confirms that multiple solutions can occur and, consequently, it is not possible to determine some of the hydraulic properties.

2.4. Experimental measurements

Because the difficulties to measure in situ 1-D downward infiltrations, the experimental validation was performed on 3-D disc infiltrometer measurements. The infiltrometer measurements were done in 10 agricultural fields located in the North Monegros county (Huesca, NE Spain). The climate is semi-arid (14.5ºC average annual temperature, 413 mm of annual average rainfall) (Comín and Williams 1994). The study area was mostly cultivated by maize, alfalfa, barley, wheat applying

sparkling irrigation and rice through flood irrigation in this quite flat area. Additional measurements on small natural shrubland areas were also performed. Textural, chemical, and management characteristics of the studied soils are summarized in Table 2.

The soil dry bulk density (ρ_b) was determined using the core method (Grossman and Reinsch, 2002) with core of 50 mm in diameter and 50 mm in height. To determine the dry weight of the soil, the samples were dried at 105ºC for 24 h. One replication, was performed per sampling site. This sampling also made it possible to determine the initial volumetric water content (θ_i) needed in Eq. (3). The 3-D transient cumulative infiltration curves were measured with a Perroux and White (1988) model tension disc infiltrometer. The diameter of applied disc and internal diameter of the water reservoir tower were 100 and 34 mm, respectively. To ensure a good contact between the soil surface and the disc base, a thin layer (< 1 cm thick) of commercial sand (80–160 μm grain size and an air-entry value between -1 and -1.5 kPa) with the same diameter as the disc base, was placed between disc and soil surface. All infiltration measurements were taken on the soil surface crust, on areas cleared of large clods and crop residue. A null pressure head on the base disc was selected. The water infiltration was automatically monitored with ±35.2 cm differential pressure transducer (Microswitch, Honeywell) applying an scanning time interval of 1 s. Infiltration measurements continued for 500 to 900 s. A soil sample was taken to estimate the saturated gravimetric water content (W) when infiltration measurement was ended. θ_s was then calculated as the product between W and the previously calculated ρ_b. A total of 10 cumulative infiltration curves were recorded. The effect of the contact sand layer on the analysis of the cumulative infiltration curve was omitted using the Latorre et al. (2015) procedure. The applied method considers the effect of sand layer as a delay in time and volume before water infiltrates into the soil. Then, the effect of the contact layer can be removed by finding the sand infiltration time (and its corresponding water volume), that corresponds to the time required for water to fill in the sand, and shifting the experimental data to the origin (in time and

water volume). Because β is directly related to the soil textural properties (Moret-Fernández and Latorre, 2017;), 0.6 for sand up to 1.7 for silt soils leading to an average β value of 1.1 was employed in the inverse analysis of the experimental infiltration curves.

3. RESULTS AND DISCUSSION

The values of S and β of the theoretical soils were numerically calculated with Eqs. (7) and (10), and Eqs. (5) and (10), respectively (Table 1). Because its greater simplicity, the effect of β on downward infiltration processes was first analysed on 1-D curves (Eq. 1). The error maps in the β-K_s, S-β and S-K_s planes showed that early infiltration times (i.e. 100 s) promoted good approaches of S but not of K_s and β (Fig. 1). The valley shapes observed in the β-K_s, S-β and S-K_s planes indicated that different combinations of K_s and β resulted in similar accuracy of infiltration curve fits (Fig. 1). However, the S-K_s error map progressively changed when longer infiltration times were applied. In this case, 1,000 s of infiltration were enough to obtain a unique and well-defined minimum in the S-K_s plane (Fig. 1), which accuracy improved with increasing infiltration times. For the remaining S-β and β-K_s planes, however, quasi-vertical and horizontal contour lines were observed (Fig. 1). This revealed that a large range of β gave similar infiltration curves, and hence S and K_s values, which indicates that β is independent of S and K_s . Only very large infiltration times (i.e. 10,000 s) allowed defining the actual β value. The small influence of β during the first stages of infiltration could be related to the fact that wetting fronts and infiltration fluxes are more related to strong water pressure gradients and less related to soil texture and thus parameter β (Moret-Fernández and Latorre, 2017) taking part in the process. However, as time increases, the water pressure head reduces and the infiltration state changes involving more the parameter β (Fig. 1). The analysis of the time-evolution of S, β and K showed that S and K_s were well defined in early and medium infiltration times, respectively. The estimation of β needed much longer time (Fig. 2). Although this simple analysis

does not allow describing the interaction between the three hydraulic parameters, it gives a fast idea of the influence of time on the optimized K_s, S and β.

Except for β, significant relationships with slope close to unity and small confidence intervals were obtained between the theoretical K_s and S and the corresponding values calculated from a global optimization over the three parameters (K_s, S and β) on a 1-D infiltration curve of 2,000 s (Fig. 3). The large confidence interval observed in β (between 0.3 and 2.0) indicates that a large range of β gives very similar infiltration curves and thus leads to comparable fits. This would indicate that β had a small effect on the downward infiltration curve and on the estimation of S and K_s. Thus, as reported by Haverkamp et al. (1994) and Latorre et al. (2015), any constant value of parameter β value can be used.

Because β does not affect the right term of the 3-D infiltration model (Eq. 2), the β-K_s, S-β and S-K_s contour maps calculated for a 3-D infiltration on a loam soil were similar to those observed in 1-D (Fig. 4). These results agree with Latorre et al. (2015), who observed that K_s and S could be accurately estimated from the inverse analysis of a 3-D downward infiltration curve when a constant β value was employed.

As an example, Figure 5 shows the experimental and the corresponding best fit infiltration curves (after removing the contact sand layer effect), and the β-K_s, S-β and S-K_s error maps calculated for the soil number 5 (Table 2). Similar to that observed for the theoretical curves, only the S-K_s error map showed a unique and well-defined minimum. In this case, 800 s of infiltration were enough to optimize these parameters. However, the quasi-vertical and horizontal contour lines obtained in the S-β and β-K_s planes indicated that a large range of β resulted in very similar S and K_s values. Thus, the great uncertainty obtained in β (Table 3) reveals that, within the range of field measurements, downward infiltration is not an appropriate technique to estimate this parameter. Finally, the significant relationship between K_s and S calculated from experimental infiltrations using a fixed β =

1.1 and those obtained by simultaneous optimization of the three hydraulic parameters (after removing the contact sand layer effect) (Fig. 6) suggests that under in situ infiltration measurements, K_s and S can be satisfactorily estimated using a constant β.

CONCLUSIONS

This work analyzes the influence of β on the cumulative infiltration curve, and the consequences on the accuracy of fits and estimates for K_s and S. The analysis was perfomed on synthetic downward infiltration generated for different times and for loam sandy, loamy and silty soils. Next the analysis was again applied on a 3-D synthetic loam curve and on experimental infiltration curves measured with a 50 mm radius disc infiltrometer. While early infiltration (i.e. 100 s) only promoted good approaches of S (Fig. 1), long infiltration times (i.e. 1,000 s) were required to estimate K_s. Only very long infiltrations (i.e. 10,000 s) allowed defining the actual β value. On the other hand, the theoretical analysis of 1-D curves indicates that β had a small effect on the downward infiltration curve, and hence, on the estimation of S and K_s. Similar behaviour was observed in the theoretical 3-D and experimental infiltration curves. Within the range of field measurements (i.e. 1000-2000 s), downward infiltration is not an appropriate procedure to estimate β. However, the saturated hydraulic conductivity and soil sorptivity can be accurately estimated using a constant β value.

Acknowledgments

This research was supported by Ministry of Economy, Industry and Innovation (CGL2014-53017-C2-1-R and CGL2016-80783-R). The authors are grateful to Área de Informática Científica of SGAI (CSIC) for their technical support in the numerical analysis, the support from ARAID Foundation and to R. Gracia and M.J. Salvador for technical help in several aspects of this study.

References

Angulo-Jaramillo R, Vandervaere JP, Roulier S, Thony JL, Gaudet JP, Vauclin, M. 2000. Field measurement of soil surface hydraulic properties by disc and ring infiltrometers. A review and recent developments. Soil Tillage Research 55: 1–29.

Ankeny, M.D., Ahmed, M., Kaspar, T.C., Horton, R., 1991. Simple field method determining unsaturated hydraulic conductivity. Soil Science Society of America Journal 55, 467-470.

Bagarello, V., Di Prima, S., Iovino, M., 2014. Comparing alternative algorithms to analyze the Beerkan infiltration experiment. Soil Sci. Soc. Am. J. 78, 724–736. http://dx.doi. org/10.2136/sssaj2013.06.0231

Carsel, R.F., R.S. Parrish. 1988. Developing joint probability distributions of soil water retention characteristics. Water Resour. Res. 24, 755-769.

Comín, F.A., Williams, W.E., 1994. Parched continents, Our common future?. In Margalef, R. (Ed.). Limnology now: A paradigm of planetary problems. Elsevier, Amsterdam, pp. 473-527.

Dane J.H., Hopmans J.W. 2002. Water retention and storage. In Methods of Soil Analysis. Part. 4, Dane JH and Topp GC (editors). SSSA Book Series No. 5. Soil Science Society of America: Madison, WI.

Di Prima, S., Lassabatere, L., Bagarello,V., Iovino, M., Angulo-Jaramillo, R. 2016. Testing a new automated single ring infiltrometer for Beerkan infilrtation experiments. Geoderma 262, 20-34.

Grossman, R.B., Reinsch, T.G., 2002. Bulk density and linear extensibility. In: Dane, J.H., Topp, G.C. (Eds.), Methods of Soil Analysis. Part 4. SSSA Book Series No. 5. Soil Science Society of America, Madison WI.

Haverkamp, R., Ross, P.J., Smettem, K.R.J., Parlange, J.Y. 1994. Three dimensional analysis of infiltration from the disc infiltrometer. Part 2. Physically based infiltration equation. Water Resour. Res., 2931-2935.

Klute, A.J. 1952. Some theoretical aspects of the flow of water in unsaturated soils. Soil Sci. Soc. Am. Proc. 16, 144-148.

Lassabatere, L., Angulo-Jaramillo, R., Soria Ugalde, J.M., Cuenca, R., Braud, I., Haverkamp, R., 2006. Beerkan Estimation of soil transfer parameters through infiltration experiments – BEST. Soil Sci. Soc. Am. J. 70, 521–532.

Lassabatere, L., Angulo-Jaramillo, R., Soria-Ugalde, J.M., Simunek, J. Haverkamp, R. 2009. Numerical evaluation of a set of analytical infiltration equations. Water Resour. Res. doi:10.1029/2009WR007941.

Latorre, B., Moret-Fernández D. 2018. A new procedure to calculate soil sorptivity, hydraulic conductivity and β parameter from a single upward infiltration. Journal of Hydrology (under review).

Latorre, B., Peña, C., Lassabatere L., Angulo-Jaramillo R., Moret-Fernández, D. 2015. Estimate of soil hydraulic properties from disc infiltrometer three-dimensional infiltration curve. Numerical analysis and field application. J. Hydrol. 57, 1-12.

Moret-Fernández, D, Latorre, B. 2017. Estimate of the soil water retention curve from the sorptivity and β parameter calculated from an upward infiltration experiment. J. Hydrol. http://dx.doi.org/10.1016/j.jhydrol.2016.11.035.

Moret-Fernández, D., Castañeda, C., Paracuellos, E., Jiménez, E., Herrero, J. 2013. Hydro-physical characterization of contrasting soils in a semiarid zone of the Ebro river valley (NE Spain). Journal of Hydrology, 486, 403-411.

Munkholm, L.J., Kay, B.D., 2002. Effect of Water Regime on Aggregate-tensile Strength, Rupture Energy, and Friability. Soil Science Society of America Journal 66, 702-709.

Parlange, J., Y. 1975. On solving the flow equation in unsaturated flow by optimization: Horizontal infiltration. Soil Sci. Soc. Am. J. 39, 415-418.

Pardalos, P.M., Romeijn, H. E. (Eds.). 2002. Handbook of global optimization (Vol. 2). Springer. Berlin.

Perroux KM, White I. 1988. Designs for disc permeameters. Soil Science Society of America Journal 52, 1205–1215.

Philip J.R. 1957. The theory of infiltration: 4. Sorptivity and algebraic infiltration equations. Soil Sci. 84, 257-264.

Pueyo, Y., Moret-Fernández, D., Saiz, H., Bueno, C.G., Alados, C.L. 2013. Relationships between plant spatial patterns, water infiltration capacity, and plant community composition in semi-arid mediterranean ecosystems along stress gradients. Ecosystems 16, 452-466.

Šimůnek, J., van Genuchten, M. Th., Šejna, M. 2006 The HYDRUS-1D software package for simulating the one-dimensional movement of water, heat, and multiple solutes in variably-saturated media. Version 3.0, *HYDRUS Software Series 1*, Department of Environmental Sciences, University of California Riverside, Riverside, CA, 270 pp.

Šimunek, J., Šejna, M., van Genuchten, M-Th. 1999. The HYDRUS-2D software package for simulating the two-dimensional movement of water, heat, and multiple solutes in variably-saturated media. Version 2.0. U.S. Salinity laboratory, Agricultural Research Service, USDA, Riverside, California.

Smettem, K.R.J., Clothier, B.E., 1989. Measuring unsaturated sorptivity and hydraulic conductivity using multi-disc permeameters. Journal of Soil Science 40, 563-568.

Smettem, K.R.J., Parlange, J.Y., Ross, P.J., Haverkamp, R., 1994. Three-dimensional analysis of infiltration from the disc infiltrometer. Part 1. A capillary-based theory. Water Resources Research 30, 2925-2929.

Van Genuchten, M.T. 1980. A closed form equation for predicting the hydraulic conductivity of unsaturated soils. Soil Sci. Soc. Am. J 44, 892– 898.

Vandervaere, J.P., Vauclin, M., Elrick, D.E., 2000. Transient Flow from Tension Infiltrometers. Part 1. The two-parameter Equation. Soil Science Society of America Journal 64, 1263-1272.

Yilmaz, D., Lassabatere, L., Angulo-Jaramillo, R., Deneele, D., Legret, M., 2010. Hydrodynamic characterization of basic oxygen furnace slag through an adapted BEST method. Vadose Zone J. 9, 107–116

Figure captions

Figure 1. Error maps for the S-β, S-K_s and β-K_s combinations calculated for a theoretical loamy soil at 100, 1000 and 10000 s of 1-D downward infiltration. The third parameter of each error map was fixed at the theoretical value. Blue symbol denotes the theoretical S, β and K values. Red contour line corresponds to Q = 0.05 mm.

Figure 2. Response surfaces for the t-S, t-K_s and t-β combinations calculated for a 1-D cumulative downward infiltration curve simulated on a theoretical loamy soil. The remaining parameters of each error map correspond to the theoretical values.Thick red line indicates the experimental uncertainty contour line (0.05 mm).

Figure 3. Relationship between the theoretical K_s and S of loamy sandy, loamy and silty soils (Table 1) and the corresponding values calculated from a global optimization over the three parameters (K_s, S and β) on a 1-D infiltration curve of 2.000 s. Vertical lines denote de confidence intervals within the 0.05 mm contour line of the error maps (Fig. 1).

Figure 4. Error maps for the S-β, S-K and β-K combinations calculated for a theoretical loamy soil at 5700 s of 3-D downward infiltration. The third parameter of each error map corresponds to the theoretical value. Blue symbol denotes the theoretical S, β and K values.

Figure 5. Experimental and the best fitting infiltration curve, and error maps for the S-β, S-K and β-K planes calculated from the 3-D downward infiltration measured in the experimental soil #5.

The third parameter of each error map was fixed at the theoretical value. Blue symbol denotes the optimized S, β and K values.

Figure 6. Relationship between K_s and S calculated from experimental infiltrations using a fixed β = 1.1 and those obtained by optimizing the three hydraulic parameters.

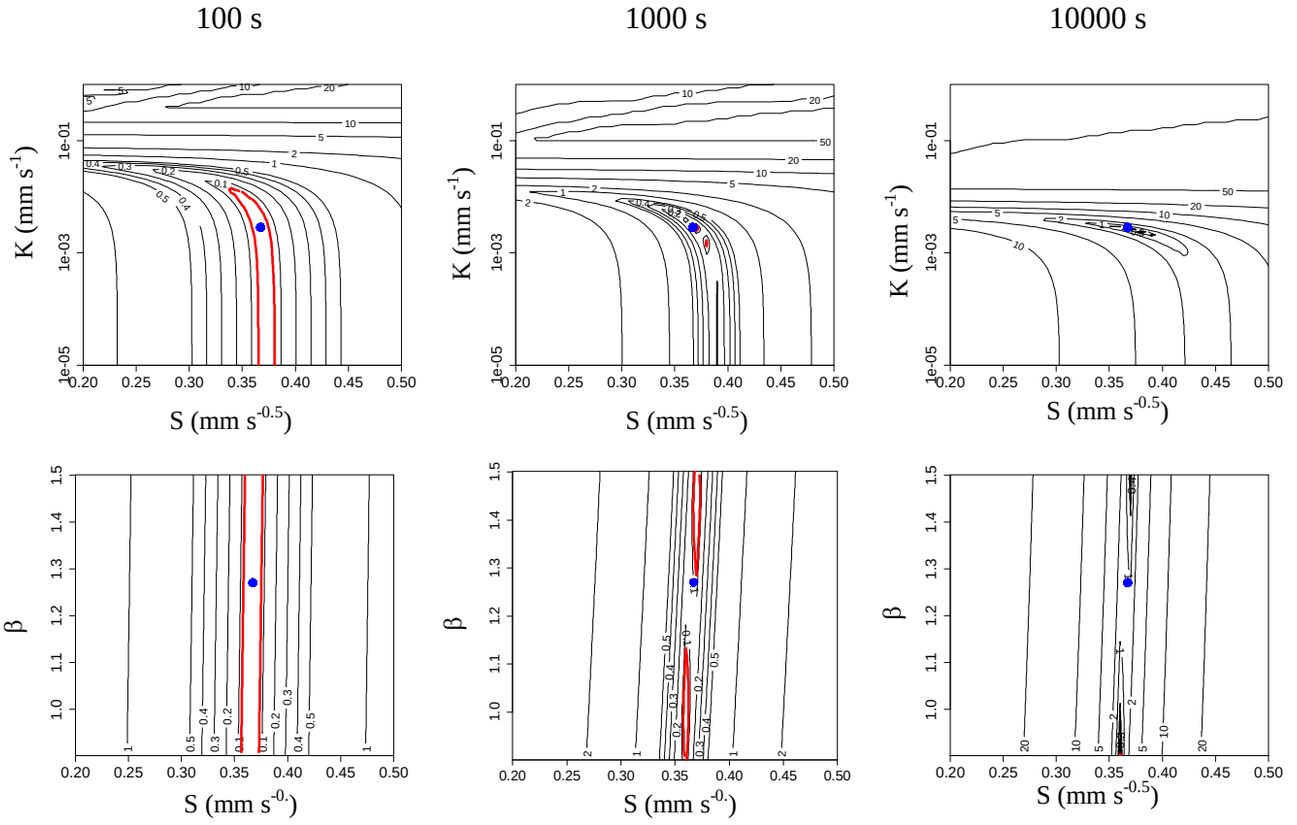

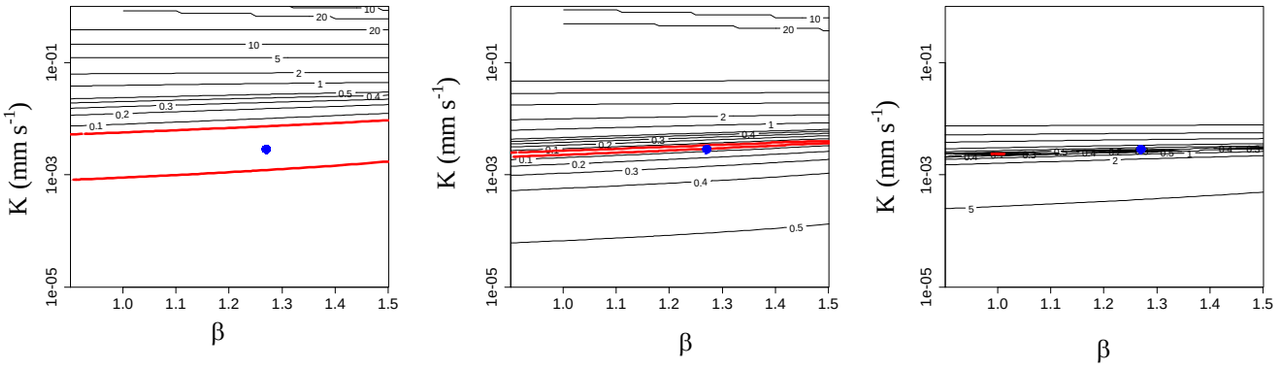

Figure 1.

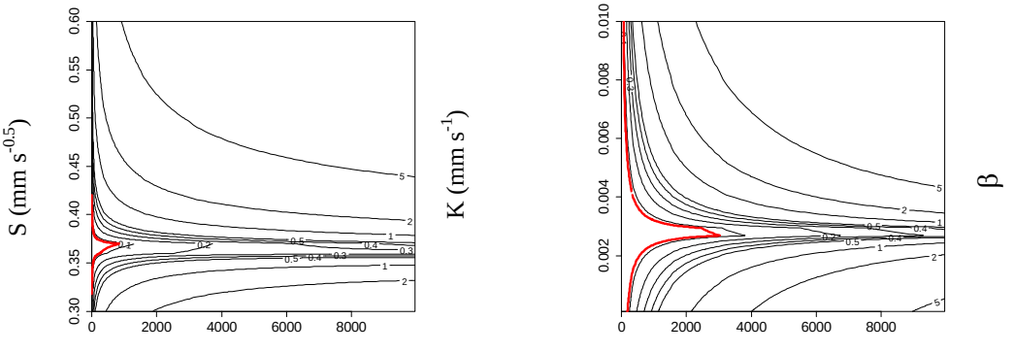

Figure 2.

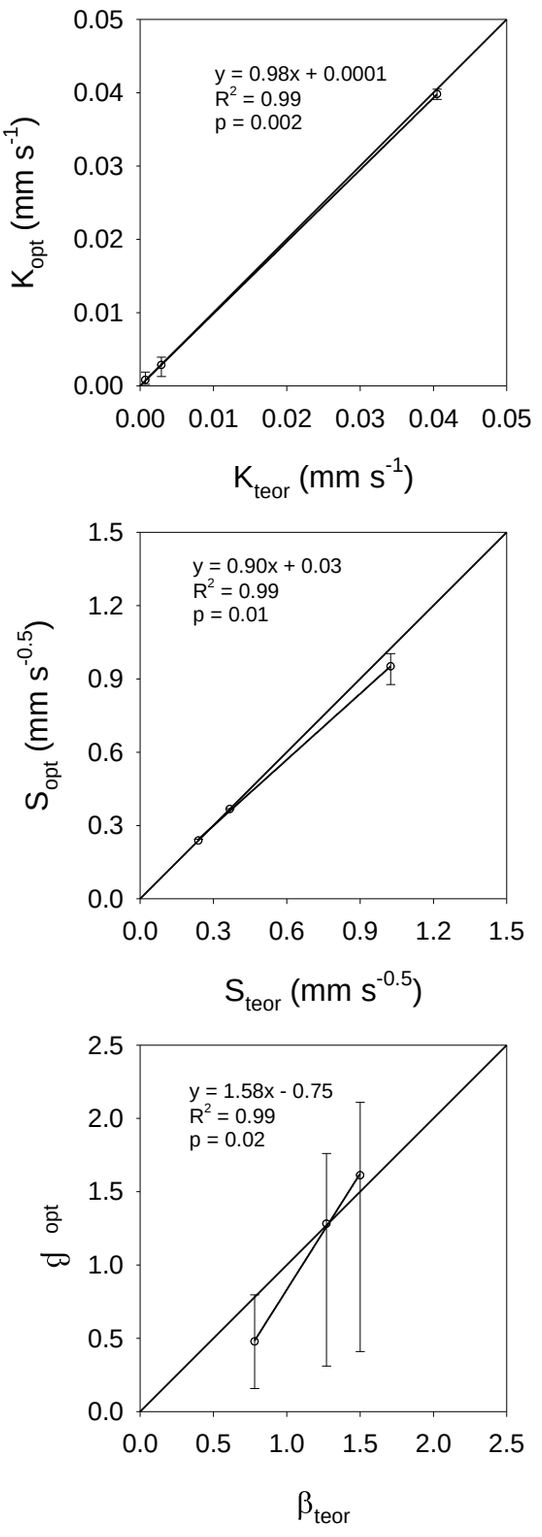
y = 0.98x + 0.0001
R2 = 0.99
p = 0.002
Kopt (mm s-1)
Kteor (mm s-1)
y = 0.90x + 0.03
R2 = 0.99
p = 0.01
Sopt (mm s-0.5)
Steor (mm s-0.5)
y = 1.58x - 0.75
R2 = 0.99
p = 0.02
β opt
βteor

Figure 3.

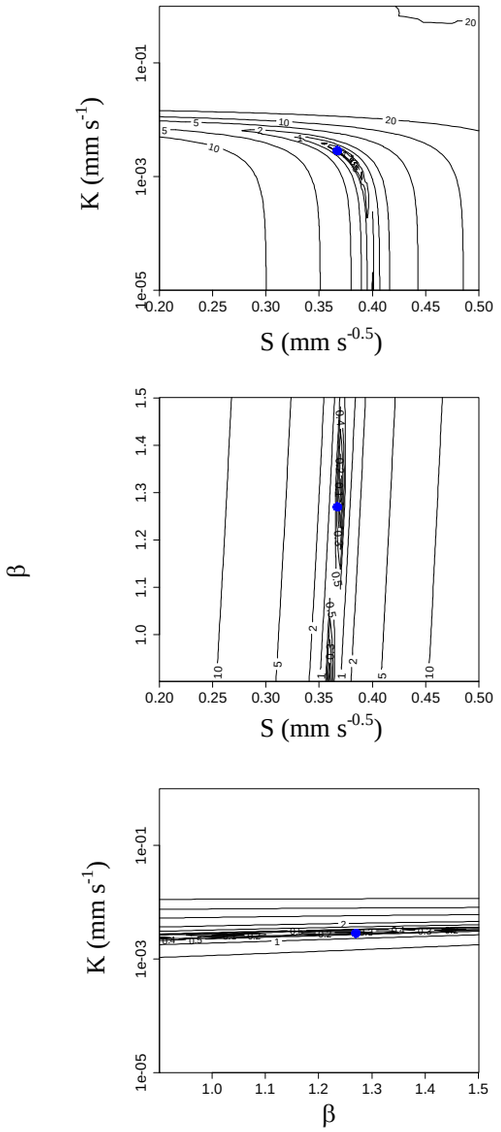
K (mm s-1)
1e-01
1e-03
1e-05
0.20
0.25
0.30
0.35
0.40
0.45
0.50
S (mm s-0.5)
β
1.0
1.1
1.2
1.3
1.4
1.5
S (mm s-0.5)
K (mm s-1)
1e-01
1e-03
1e-05
1.0
1.1
1.2
1.3
1.4
1.5
β

Figure 4.

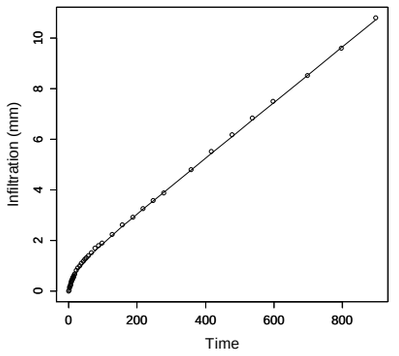
Infiltration (mm)
Time
0
2
4
6
8
10
0
200
400
600
800

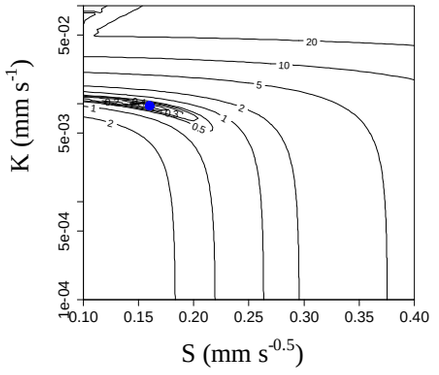
K (mm s-1)
S (mm s-0.5)
1e-04
5e-04
5e-03
5e-02
0.10
0.15
0.20
0.25
0.30
0.35
0.40

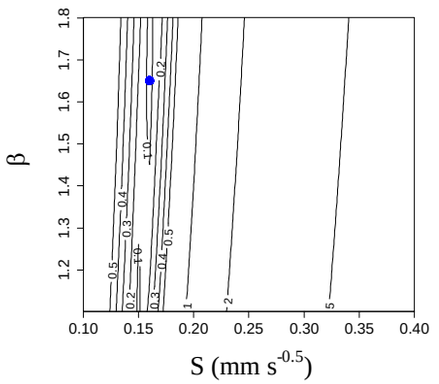
β
S (mm s-0.5)
1.2
1.3
1.4
1.5
1.6
1.7
1.8
0.10
0.15
0.20
0.25
0.30
0.35
0.40

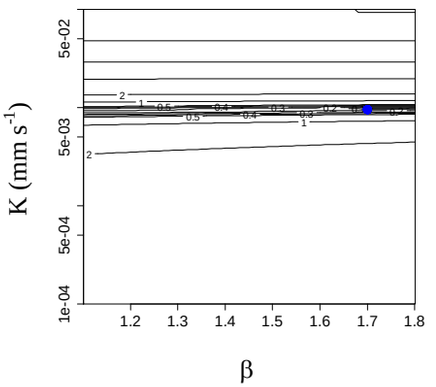
K (mm s-1)
β
1e-04
5e-04
5e-03
5e-02
1.2
1.3
1.4
1.5
1.6
1.7
1.8

Figure 5.

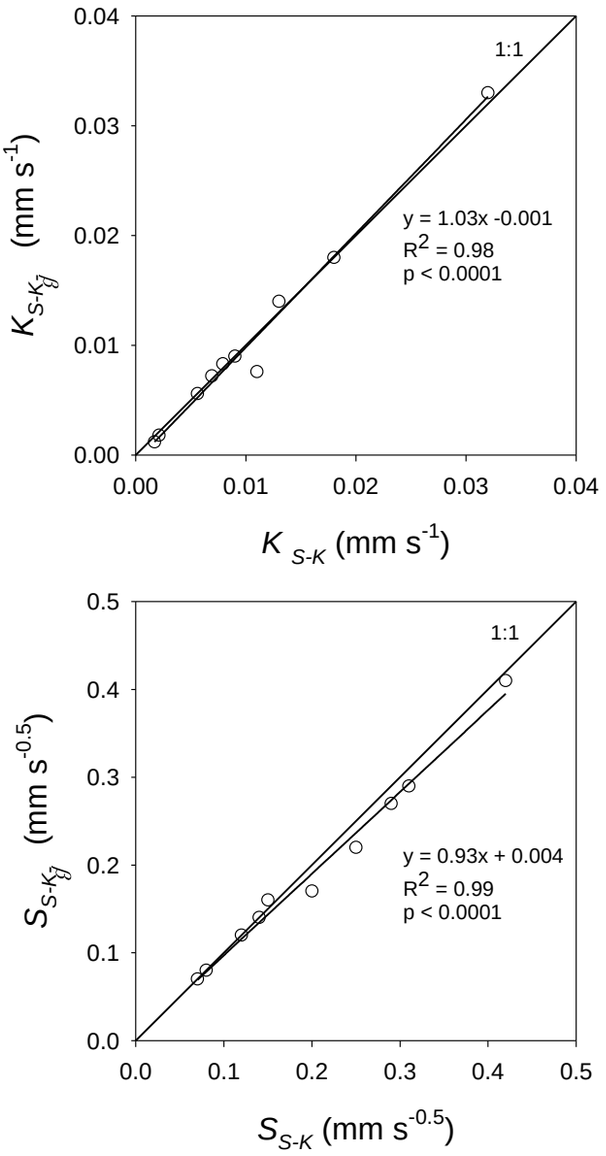

Figure 5.

Table 1. Values of initial (θ_i), saturated (θ_s) and residual (θ_r) water content, α and n parameters of the van Genuchten (1980) water retention curve, hydraulic conductivity (K_s) and sorptivity (S) (Eq. 8) at saturation and shape factor (β) (Eq. 3) of the theoretical loamy sand, loam and silt soils.

	θ_i	θ_s	θ_r	α	n	K_s	S	β
	$cm^3\ cm^{-3}$			cm^{-1}		$mm\ s^{-1}$	$mm\ s^{-0.5}$	
Loamy sand	0.057	0.41	0.057	0.124	2.28	$4.05\ 10^{-2}$	1.025	0.78
Loam	0.078	0.43	0.078	0.036	1.56	$2.88\ 10^{-3}$	0.367	1.27
Silt	0.034	0.46	0.034	0.016	1.37	$6.93\ 10^{-4}$	0.238	1.50

Table 2. Soil $CaCO_3$,organic carbon (OC) and initial (θ_i) and saturated (θ_s) volumetric water contents, soil bulk density, ρ_b, soil texture and soil management characteristics of the studied soils.

Soil number	$CaCO_3$	OC	θ_i	θ_s	ρ_b	Sand	Silt	Clay	Soil and use management
	g kg^{-1}		m^3 m^{-3}			%			
1	185	6.33	0.1	0.37	1.45	83.73	14.27	2.00	Agricultural (under fallow in a cereal-fallow rotation with conventional tillage)
2	244	9.88	0.22	0.37	1.45	50.44	36.29	13.28	Agricultural (rainfed cereal cropping under no tillage)
3	308	9.74	0.12	0.50	1.64	47.92	36.77	15.31	Agricultural (rainfed cereal cropping under conventional tillage)
4	269	5.34	0.06	0.43	1.46	55.47	32.08	12.45	Agricultural (irrigated cereal cropping under conventional tillage)
5	350	12.77	0.15	0.467	1.50	48.25	35.95	15.80	Agricultural (rainfed cereal cropping under no tillage)
6	208	10.26	0.06	0.54	1.41	50.73	37.68	11.59	Agricultural (irrigated legume crop under conventional tillage)
7	265	18.50	0.05	0.54	1.27	44.48	39.18	16.34	Agricultural (irrigated legume crop under conventional tillage)
8	237	13.18	0.02	0.54	1.17	55.60	31.69	12.71	Agricultural (rainfed cereal cropping under no tillage)
9	419	36.68	0.06	0.55	0.82	46.67	33.31	20.02	Natural (typical Mediterranean shrubland)
10	257	15.23	0.26	0.55	1.35	25.87	49.79	24.34	Agricultural (irrigated cereal cropping under conventional tillage)

Table 3. Hydraulic conductivity (K_s), sorptivity (S) and β factor estimated from the inverse analysis of experimental 3-D cumulative infiltration curves using the Latorre et al. (2015) procedure (with a fixed β) and optimizing the three hydraulic parameters. Within brackets, the confidence interval within the 0.05 mm error contour line

Soil	K_s and S optimization (Latorre et al., 2015)			K_s, S and β optimization		
	K_s	S	β	K_s	S	β
	mm s^{-1}	mm $s^{-0.5}$		mm s^{-1}	mm $s^{-0.5}$	

1	$1.1\ 10^{-2}$ [$7.7\ 10^{-3}$, $4.4\ 10^{-2}$]	0.42 [0.42, 0.43]	1.1	$7.6\ 10^{-3}$ [$7.5\ 10^{-3}$, $1.9\ 10^{-2}$]	0.41 [0.41, 0.42]	0.18 [0.18, 1.89]
2	$3.2\ 10^{-2}$ [$3.2\ 10^{-2}$, $3.3\ 10^{-2}$]	0.25 [0.24, 0.26]	1.1	$3.3\ 10^{-2}$ [$3.3\ 10^{-2}$, $3.4\ 10^{-2}$]	0.22 [0.20, 0.23]	0.76 [0.73, 1.31]
3	$5.6\ 10^{-3}$ [$5.1\ 10^{-3}$, $6.5\ 10^{-3}$]	0.08 [0.08, 0.10]	1.1	$5.6\ 10^{-3}$ [$5.0\ 10^{-3}$, $6.3\ 10^{-3}$]	0.08 [0.07, 0.09]	0.97 [0.30, 2.00]
4	$1.7\ 10^{-3}$ [$1.0\ 10^{-3}$, $2.4\ 10^{-3}$]	0.07 [0.06, 0.08]	1.1	$1.2\ 10^{-3}$ [$1.1\ 10^{-3}$, $2.7\ 10^{-3}$]	0.07 [0.06, 0.07]	0.18 [0.18, 2.00]
5	$9.0\ 10^{-3}$ [$0.9\ 10^{-3}$, $1.0\ 10^{-3}$]	0.15 [0.15, 0.16]	1.1	$9.0\ 10^{-3}$ [$0.9\ 10^{-3}$, $1.0\ 10^{-3}$]	0.16 [0.16, 0.17]	2.11 [1.57, 2.11]
6	$2.1\ 10^{-3}$ [$1.4\ 10^{-3}$, $2.9\ 10^{-3}$]	0.12 [0.12, 0.13]	1.1	$1.8\ 10^{-3}$ [$1.2\ 10^{-3}$, $3.6\ 10^{-3}$]	0.12 [0.12, 0.13]	0.69 [0.30, 2.00]
7	$1.8\ 10^{-2}$ [$1.8\ 10^{-2}$, $1.9\ 10^{-2}$]	0.31 [0.31, 0.32]	1.1	$1.8\ 10^{-2}$ [$1.8\ 10^{-2}$, $1.9\ 10^{-2}$]	0.29 [0.29, 0.30]	0.74 [0.46, 0.92]
8	$7.9\ 10^{-3}$ [$7.9\ 10^{-3}$, $8.7\ 10^{-3}$]	0.20 [0.19, 0.21]	1.1	$8.3\ 10^{-3}$ [$7.1\ 10^{-3}$, $9.4\ 10^{-3}$]	0.17 [0.17, 0.18]	0.64 [0.30, 1.37]
9	$1.3\ 10^{-2}$ [$1.3\ 10^{-2}$, $1.4\ 10^{-2}$]	0.29 [0.28, 0.31]	1.1	$1.4\ 10^{-2}$ [$1.1\ 10^{-2}$, $1.4\ 10^{-2}$]	0.27 [0.28, 0.29]	0.85 [0.30, 1.18]
10	$6.9\ 10^{-3}$ [$6.5\ 10^{-3}$, $8.2\ 10^{-3}$]	0.14 [0.13, 0.16]	1.1	$7.2\ 10^{-3}$ [$6.7\ 10^{-3}$, $8.4\ 10^{-3}$]	0.14 [0.13, 0.15]	0.41 [0.30, 1.33]

This work analyses the influence of the β on the estimate of K and S

Early infiltration times (i.e. 100 s) promoted good estimations for S

Longer infiltrations (i.e. 1.000 s) were required to estimate accurately K_s

Only very long infiltration (i.e. 10.000 s) allowed defining the actual β value

S and K_s can be accurately estimated using a constant β